Environmental Science and Ecotechnology 29 (2026) 100664

Contents lists available at ScienceDirect

Environmental Science and Ecotechnology

journal homepage: www.journals.elsevier.com/environmental-science-and-ecotechnology/

Original Research

Scaled decentralization for sustainable wastewater treatment in high-density cities

Aliya Abulimiti [a,b], Boxuan Wang [a,b], Xiuheng Wang [a,b,*], Nanqi Ren [a,b]

[a] State key Laboratory of urban Water Resource and Environment, Harbin Institute of Technology, Harbin, 150090, China
[b] School of Environment, Harbin Institute of Technology, Harbin, 150090, China

ARTICLE INFO

Article history:
Received 31 May 2025
Received in revised form
28 January 2026
Accepted 28 January 2026

Keywords:
Scaled decentralized systems
Life cycle assessment
Scale
Wastewater treatment technologies
Resource recovery

ABSTRACT

Sustainable urban wastewater management requires systems that effectively remove pollutants while enabling resource recovery and diminishing environmental impacts. In high-density cities, conventional centralized treatment plants often entail long conveyance distances, high pumping energy, and substantial methane emissions from widespread communal septic tanks, compounded by stringent effluent standards. Scaled decentralized systems (SDSs)—distributed facilities integrated into existing sewer networks—offer potential advantages through reduced transport and localized recovery, yet their performance across scales, technologies, and recovery strategies remains poorly quantified. Here we show that SDSs featuring 20,000 m^3 d^{-1} moving-bed biofilm reactor plants with combined water reuse and additional heat-pump energy recovery achieve the lowest life-cycle environmental impacts and costs. We applied whole-system life-cycle assessment and cost analysis of 29 scenarios treating 100,000 m^3 d^{-1} of wastewater in a city in China. These configurations reduce global warming potential by up to 52.5% relative to an optimized centralized benchmark, owing to shorter sewers that preserve influent carbon for biological denitrification, elimination of external carbon dosing, and efficient dual recovery; upstream septic tanks, however, contribute 24–47% of total warming potential, highlighting a key trade-off. These findings demonstrate that carefully scaled decentralization, paired with robust biofilm technology and integrated recovery, provides a superior pathway for sustainable wastewater infrastructure in dense urban settings.

1. Introduction

For over a century, centralized wastewater treatment systems, fundamental to urban sanitation, have directed wastewater via extensive pipe networks to large-scale wastewater treatment plants (WWTPs) [1]. These facilities typically serve populations from thousands to millions of population equivalents and require a large capital investment [2]. Historically, factors such as extensive land requirements, technical challenges (e.g., odor control), and public opposition ("not-in-my-backyard" concerns) favored siting these plants distantly downstream [3,4].

China exemplifies this trend, rapidly adopting a centralized model to develop one of the world's largest wastewater sectors [5]. Official data reveal that urban wastewater treatment volume has risen from 12 billion m^3 in 2001 to 55.7 billion m^3 in 2020, with a 97.5% treatment rate [6]. This rapid expansion based on large WWTPs represents a significant public health achievement. However, the legacy of these systems—whose locations often reflect historical urban boundaries, which are now surpassed by city growth—presents inherent sustainability challenges. High energy demands for treatment and pumping, coupled with logistical barriers to resource recovery (water, energy, nutrients), challenge the long-term viability and circular-economy potential [7]. Consequently, stricter environmental regulations and the pursuit of the United Nations' (UN) sustainable development goals (SDGs) highlight the need for alternative wastewater strategies in megacities [8].

Recognition of these challenges has driven the exploration of alternative paradigms, particularly decentralized and distributed systems, ranging from on-site to cluster scale [9]. Among these, source separation systems achieve high recovery by separately

* Corresponding author. State key Laboratory of urban Water Resource and Environment, Harbin Institute of Technology, Harbin, 150090, China.
E-mail address: xiuheng@hit.edu.cn (X. Wang).

https://doi.org/10.1016/j.ese.2026.100664

collecting and treating waste streams [10]. However, such systems often require dual piping and major retrofits, which are particularly difficult in regions with established centralized infrastructure [11], such as China. Scaled decentralized systems (SDSs) represent a feasible intermediate approach in sustainable urban wastewater management [12]. Unlike purely onsite units, SDSs are distributed facilities integrated into existing sewer networks to serve community- or district-scale catchments, thus reducing conveyance distances while maintaining robust treatment performance [13]. Guided by the principle "as small as possible, as large as necessary," they balance the economies of scale of large plants with the localized resource recovery potential of smaller units. For high-density urban areas that generate approximately 100,000 m^3 d^{-1} of wastewater (typically serving several hundreds of thousands of residents), recent studies recommend scaled decentralization using multiple 10,000–20,000 m^3 d^{-1} facilities [12].

Applying this SDS concept in China requires confronting a unique infrastructural legacy: the communal septic tank. Unlike standalone septic tanks in detached dwellings in the United States—which combine settling with infiltration or leach fields—Chinese communal septic tanks are embedded in sewer networks for preliminary treatment, typically serve 200–300 residents per unit (equivalent to 1–2 residential buildings), and provide a hydraulic retention time of 12–24 h [14]. Extensively built over previous decades under regulatory mandates, they persist as an enduring element of urban infrastructure. Their persistence and environmental relevance—particularly methane (CH_4) emissions [15]—imply that communal septic tanks should be considered when evaluating SDSs in China.

SDSs can integrate with these localized collection infrastructures, with plants enabling technologies such as membrane bioreactors (MBR), constructed wetlands (CW), and moving bed biofilm reactors (MBBR) [16]. These technologies are specifically selected to meet the widely implemented discharge standard, Class A, in China, which requires the effluent to meet the reclaimed water level. They also support localized resource recovery, such as water reuse (WR) and heat pump (HP) energy extraction, due to proximity to the demand nodes [17]. Life cycle assessment (LCA) provides a comprehensive framework to evaluate these system transitions [18]. However, most studies compare small, decentralized units with large, centralized systems, often beyond the Chinese urban context [19]. Previous assessments have considered configurations, such as septic tanks alone [20], septic tanks combined with CW [19], standalone MBR systems [21], or urine-separation hybrids [18]. The results of these assessments reveal complex trade-offs: decentralized systems can reduce sewer infrastructure [19,20] and enhance local recovery, while centralized systems may perform better in ecosystem quality due to better-managed air emissions and discharges [20]. These divergent findings often stem from heterogeneous methodological choices—for example, whether to include sewer network construction, how to credit resource recovery, or which functional unit to apply—thereby making cross-study comparisons difficult and underscoring the need for context-specific evaluations [22]. Importantly, comprehensive LCA of intermediate-scale SDSs within the unique context of China's high-density, septic tank-integrated urban infrastructure remains limited, particularly with regard to optimal scale and technology selection and the comprehensive optimization of resource recovery strategies (including HP-based energy recovery).

This study employed LCA to evaluate the economic and environmental performance of a conventional centralized baseline and several SDS configurations in a high-density urban context. The SDS configurations examined range from 5000 to 20,000 m^3 d^{-1} per facility, deploying 5–20 distributed plants using MBR, CW, or MBBR technologies. The analysis adopted a full process-chain perspective, explicitly accounting for upstream septic tank impacts, wastewater conveyance, plant operation (based on detailed process inventories and mechanistic modeling), and sludge management. Resource recovery options—including WR, HP, and nutrient recycling—were systematically assessed. By quantifying system-wide lifecycle impacts, this study identifies trade-offs among SDS scales, technologies, and recovery pathways, and assesses their integration with existing infrastructure.

2. Method

2.1. Scenario definitions

Three SDS configurations, differing in terms of their WWTP scale (individual facility capacity) and degree of distribution (number of facilities), were evaluated and compared against a centralized baseline (Fig. 1). The baseline represents the current regional practice: a single 100,000 m^3 d^{-1} WWTP, designated as the conventional centralized system (CS) configuration. The SDS configurations distribute this capacity across smaller facilities integrated into the urban network: (1) SDS20—each plant with a capacity of 20,000 m^3 d^{-1}, with five facilities; (2) SDS10—each plant with a capacity of 10,000 m^3 d^{-1}, with 10 facilities; (3) SDS5: each plant with a capacity of 5000 m^3 d^{-1}—with 20 facilities. All configurations serve the same 38.4 km^2 study area in Northern China, accommodating 315,000 people (average per capita water use: 271 l d^{-1}). The total generated wastewater load from this population remains constant across all configurations, as does the total design treatment capacity (100,000 m^3 d^{-1}). To ensure comparable influent quality, contributions from industrial wastewater, stormwater, and sewer leakage were excluded [23].

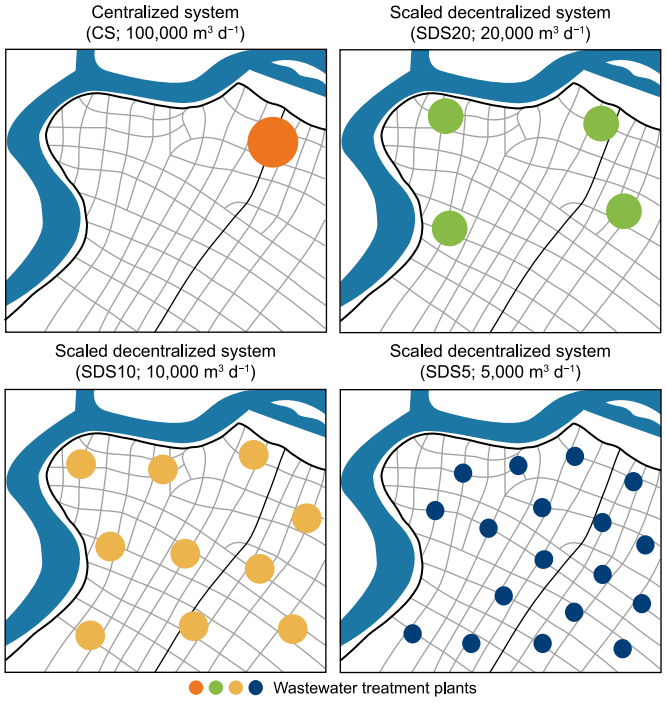

Fig. 1. Conceptual configurations for centralized system (CS) and scaled decentralized systems (SDSs). The baseline represents the current regional practice: a single wastewater treatment plant with a capacity of 100,000 m^3 d^{-1}. The SDS configurations includes SDS5 (each plant with a capacity of 5000 m^3 d^{-1}, 20 facilities), SDS10 (each plant with a capacity of 10,000 m^3 d^{-1}, 10 facilities), and SDS20 (each plant with a capacity of 20,000 m^3 d^{-1}, 5 facilities).

This case study focused on the 5000–20,000 m^3 d^{-1} WWTP scale range to capture the economics of treatment technology in high-density cities with Class A discharge requirements, i.e., stringent effluent quality limits for key pollutants (GB 18918-2002). WWTPs below 5000 m^3 d^{-1} often face reduced energy efficiency [24], whereas WWTPs above 10,000 m^3 d^{-1} achieve economies of scale [13]. However, SDS configurations at larger WWTP scales increasingly resemble centralized systems due to their reduced distribution, thereby diminishing some decentralization benefits (e.g., reduced sewer network requirements, lower conveyance energy use, and enhanced local water reuse/resource recovery) [25].

2.2. Conventional centralized wastewater treatment system

2.2.1. Sewer network design and influent characterization

In the CS configuration, wastewater first passes through communal septic tanks and is then conveyed to the centralized WWTP through the sewer network (Fig. 2a). These tanks, integrated into the municipal sewer network as preliminary treatment units, typically provide a hydraulic retention time of 0.8 days (Supplementary Text S1).

The sewer network connecting the communal septic tank to the WWTP was designed using Hongye Equipment Design Water Supply and Drainage software, which implements methodologies from drainage engineering and national design codes. The network is a gravity-based separate sewer system that excludes rainwater and sewer leakage, thus ensuring the integrity of wastewater flow and pollutant load data [26]. Two intermediate pumping stations help handle the area's terrain (Supplementary Text S1). The hydraulic characteristics of each pipeline, including pipeline segment length, internal diameter, slope, and filling ratio, are summarized (Supplementary Table S1).

Pollutant transformations within the network were explicitly modeled to characterize the influent quality reaching the WWTP after being transported through the extensive conveyance system. A first-order kinetic model was applied segment-by-segment to estimate changes in pollutant concentration during conveyance. While more complex mechanistic models for sewer degradation are available, the present study only requires an overall transformation rate constant (k) to represent the combined net effects of in-sewer processes [27]. Accordingly, the first-order model provides a reasonable approximation of net pollutant transformation for LCA purposes. The robustness of this assumption and its influence on overall conclusions were subsequently evaluated through a sensitivity analysis.

Site-specific k values for chemical oxygen demand (COD), total phosphorus (TP), and ammonium nitrogen (NH_4^+-N) were estimated from a 15-day continuous field sampling campaign (26 April–10 May 2024). Under dry-weather conditions, samples were collected simultaneously at septic tank outlets (network inlets) and the WWTP inlet (network outlet). At each location, hourly samples were drawn using submersible pumps and composited into daily 24-h averages in equal volumes. These paired inlet–outlet concentrations were then used to back-calculate k for the entire sewer network.

Based on measured concentrations and the length of each pipeline segment (L) of the network, k values were derived using equation (1):

$$\frac{dC}{dL} = -kC \tag{1}$$

where C is the pollutant concentration at a given point along the pipeline (mg L^{-1}), and k is the transformation rate constant (km^{-1}).

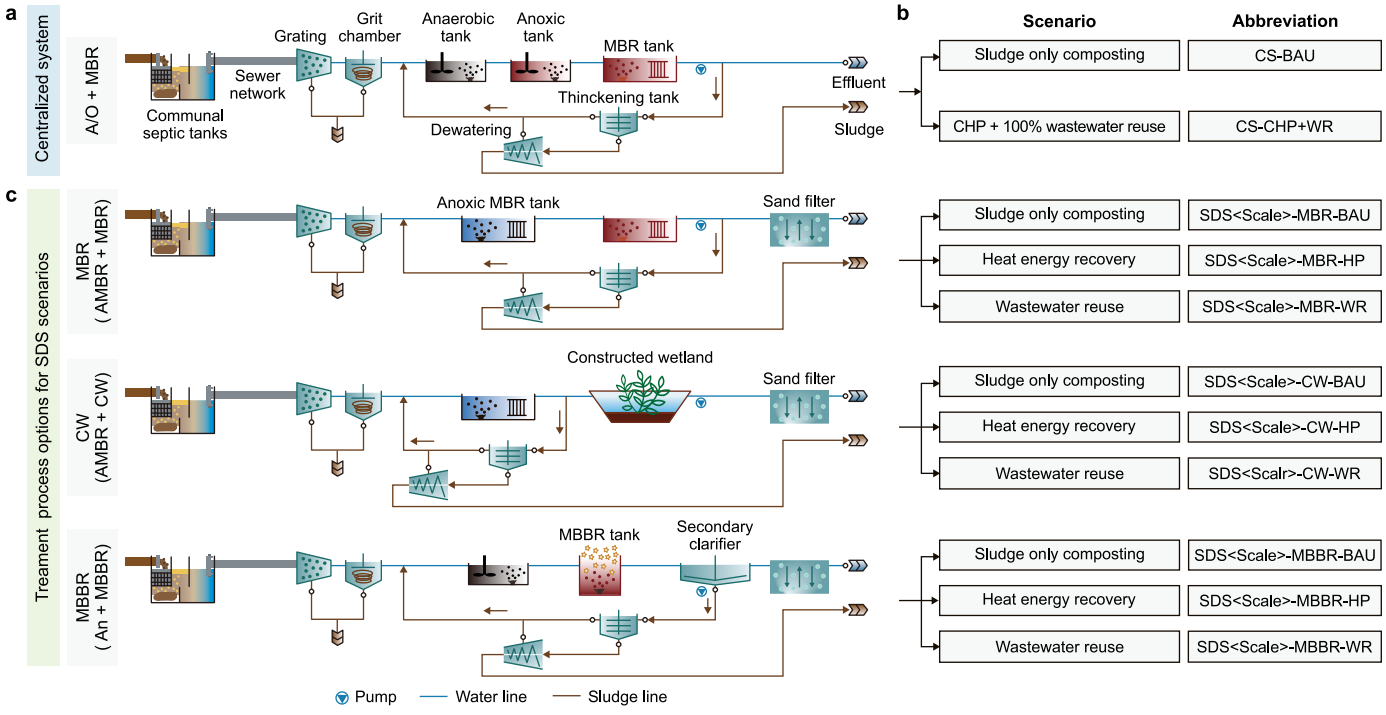

Fig. 2. Treatment configurations and evaluated scenarios. a, Process flow for the centralized system (CS). **b**, Overview of all evaluated scenarios, including CS and scaled decentralized system (SDS) configurations, with the associated treatment technologies and resource-recovery options. **c**, Process flow diagrams for the treatment technologies implemented in the SDS configurations: membrane bioreactor (MBR), constructed wetland (CW), and moving bed biofilm reactors (MBBR). Definitions: CHP, combined heat and power. HP, heat pump. WR, water reuse. BAU, business-as-usual. An, anaerobic tank. AMBR, an anoxic MBR.

The sewer network is a dendritic (tree-like) structure with multiple trunks and main segments. The back-calculated k values (Supplementary Table S2) were applied segment-by-segment: at each pipe segment, concentrations were transformed according to equation (1); at confluence points, concentrations were recalculated using mass conservation principles before continuing to the next segment (detailed calculation procedure in Supplementary Text S1). The first-order kinetic model, a core component of this approach, is mechanistically justified and validated (Supplementary Text S1 and Figs. S1–S3). The final concentrations at the WWTP inlet, determined through this sequential segment-by-segment modeling, defined the influent characteristics. These k values were subsequently applied to all evaluated scenarios (CSs and SDSs), with scenario-specific influent concentrations calculated based on each scenario's conveyance distance.

2.2.2. Centralized WWTP simulation

The operational performance of the centralized WWTP was characterized through steady-state simulations using SUMO software (Dynamita). The modeled core treatment process is an anaerobic/oxic (A/O) activated sludge system with tertiary MBR separation (Supplementary Fig. S4 and Table S3).

The SUMO platform, which incorporates mechanistic models of microbial processes such as organic matter oxidation and nitrification–denitrification, was utilized to generate robust greenhouse gas (GHG) emission inventories, including nitrous oxide (N_2O), CH_4, and fossil carbon dioxide (CO_2), as these are not available from routine plant monitoring. The model underwent steady-state calibration to ensure its reliability; it achieved robust quantitative alignment with measured effluent and operational energy data from the existing regional WWTP [28], as evidenced by low relative errors for key parameters (typically within ±10%). The detailed design and calibration process, including key parameters and performance comparisons (Supplementary Text S1, and Tables S4 and S5). The SUMO simulation in this study primarily generated representative LCA inventory data, consistent with LCA's steady-state requirements for assessing average performance.

2.2.3. Resource recovery scenarios for CS configuration

For the CS configuration, two evaluated scenarios were defined; each was predicated on a distinct resource recovery option (Fig. 2b):

(i) CS-BAU: A baseline scenario in which treated effluent is discharged into receiving rivers due to the long distance for pumping back to the dwellings, and dewatered sludge undergoes aerobic composting for land application.
(ii) CS-CHP + WR: An enhanced recovery scenario featuring sludge anaerobic digestion with combined heat and power (CHP) for energy recovery, and reuse of treated wastewater for industrial cooling, landscape irrigation, and other applications. Digestate is subsequently composted.

2.3. Scaled decentralized systems

2.3.1. Sewer network configuration and influent characterization

For each SDS configuration (SDS5, SDS10, and SDS20), the baseline sewer network was adjusted and reorganized through pipeline restructuring and throttling, thus ensuring efficient service for the respective number of facilities while maintaining consistent design principles. Existing communal septic tanks were preserved within the network to provide preliminary treatment, which effectively removes settleable solids and reduces the organic load, thereby reducing pressure on downstream pipelines and treatment facilities. Detailed sewer network design parameters and corresponding transport energy estimates are provided (Supplementary Text S2 and Tables S6–S9).

Pollutant variation within the network was calculated using the transformation rate constants determined in Section 2.2.1. The reorganized network structures and shortened conveyance distances in SDSs reduce in-sewer biochemical reactions, sedimentation, and gas losses [29], thereby resulting in influent to SDS WWTPs with higher COD concentrations and altered nutrient characteristics compared with long centralized sewers. The influent COD/total nitrogen (TN) ratios increased from 8.2 (CS) to 9.6 (SDS5), 9.4 (SDS10), and 9.0 (SDS20). This enabled the estimation of the final influent quality for each SDS configuration. The resulting influent quality serves as a key input for designing the downstream treatment processes. Final influent pollutant concentrations are detailed in Supplementary Text S2 and Table S10.

2.3.2. SDSs technology selection and process design

Three wastewater treatment technologies were evaluated for the SDS configurations—MBR, CW, and MBBR—selected for their suitability across SDS5, SDS10, and SDS20 scales (Fig. 2c). Each technology defines the core process for specific SDS scenarios.

MBR (AMBR + MBR). MBR technology offers high process stability, a compact footprint, potential for water reuse, and reduced sludge production compared to a conventional activated sludge system [30]. To enhance TN removal and meet Class A discharge standards, an anoxic MBR (AMBR) tank precedes the aerobic MBR, which is followed by sand filtration. Design and operational details are provided in Supplementary Tables S11 and S12.

CW (AMBR + CW). CWs are ideal for SDSs due to their low maintenance requirements, operational simplicity, minimal sludge production, and cost-effectiveness [31]. However, CWs alone may not meet COD and TN discharge standards. Integrating an AMBR with a CW enhances treatment efficiency, particularly for nitrogen removal [32]. In this study, an AMBR was integrated with a vertical subsurface flow CW, followed by sand filtration, to ensure compliance with Class A discharge standards. Design details follow technical guidance in China (Supplementary Tables S13 and S14).

MBBR (An + MBBR). MBBR utilizes biofilms on carriers (e.g., high-density polyethylene (HDPE) plastic carriers) for efficient organic and nutrient removal, with enhanced nitrogen removal via extended sludge retention [33]. The high biomass concentration, enabled by carriers' large surface area, suits space-limited urban settings [34]. This study employs an anaerobic tank (An) and aerobic MBBR, followed by secondary sedimentation and sand filtration. Design parameters are detailed in Supplementary Tables S15 and S16.

Each technology was modeled using SUMO for SDS5, SDS10, and SDS20 scales, thus ensuring a consistent framework for performance comparison. Steady-state simulations, based on scale-specific influent characteristics (Section 2.3.1), generated comprehensive LCA inventory data for these conceptual SDS designs, thus predicting effluent quality, energy consumption, and direct GHG emissions. All processes achieved Class A effluent standards under the specified conditions (Supplementary Text S2).

2.3.3. Resource recovery scenarios for SDSs

Building on the three distinct wastewater treatment technologies (MBR, CW, and MBBR) introduced in Section 2.3.2, each was systematically applied and evaluated across all three SDS scales (SDS5, SDS10, and SDS20). Thereafter, for every resulting technology-scale combination, we defined various resource recovery scenarios.

Sludge from small-scale SDS plants, in limited quantities, is transported to a central aerobic composting facility. Due to their urban proximity, SDSs enable efficient heat recovery via HPs for building heating or cooling, thereby leveraging their localized nature to enhance energy efficiency. In contrast, centralized plants in suburban areas are less suitable for heat recovery due to their distance from urban heat demand centers. We defined the following resource recovery scenarios (Fig. 2b):

(1) BAU: Sludge composting with direct discharge of treated wastewater;
(2) HP: Heat recovery via HPs from treated effluent, with composted sludge;
(3) WR: Reuse of treated wastewater for irrigation or street cleaning, with sludge composted.

SDS scenarios are subsequently denoted using the format SDS<scale>−<technology>−<recovery>. In this format, "scale" is 5, 10, or 20 (representing SDS5, SDS10, and SDS20, respectively); "technology" is MBR, CW, or MBBR; and "recovery" is BAU, HP, or WR. For example, SDS5-MBR-HP represents an evaluated scenario based on the SDS5 scale, thus employing MBR technology with HP recovery.

Combining three technologies, three scales, and three recovery options yields 27 SDS scenarios. These, along with two centralized system scenarios (CS-BAU and CS-CHP + WR), form a matrix of 29 configurations for comparison. Following the primary assessment of these 29 scenarios, a combined resource recovery strategy (WR + HP) was evaluated for the most promising SDS configuration to investigate potential synergistic benefits. The methodology for energy recovery calculations is detailed in Supplementary Text S3 and Tables S17–S18.

2.4. Life cycle assessment method

2.4.1. Goals and scope

The system boundaries encompassed the entire process, from communal septic tank treatment to the sewer network, wastewater treatment, sludge disposal, and resource recovery stages (Fig. 3). Decommissioning was excluded due to its minimal impact and limited data availability [30]. The functional unit for all scenarios was the collection and treatment of 1 m^3 of wastewater. To ensure comparability, all scenarios were designed to meet the Class A discharge standard, and water volume losses during treatment were assumed negligible. System lifespans were set at 50 years for septic tanks, sewer networks, and WWTPs [21]. Component replacement cycles were 15 years for pumps and blowers, 5 years for membranes, and 25 years for biofilm media [35].

2.4.2. Life cycle inventory

We considered the construction phase for all system components (Fig. 3). A transport distance of 20 km was assumed for construction materials. Infrastructure material inventories were primarily derived from bills of quantities (BoQ) in actual engineering project reports (2018–2022) provided by a leading municipal design institute in China, with each evaluated configuration (WWTP scale/technology, sewer network scale) corresponding to actual design cases or representative projects. Missing data—particularly for CWs, septic tanks, CHP, HP systems, and major equipment—were supplemented by the literature [17,21,36,37]. Detailed data sources and acquisition methods are documented in Supplementary Text S4 and Table S19.

The operational phase included energy consumption, chemical use, and emissions from gases, wastewater, and solid waste (Fig. 3). We derived septic tank operation data from published literature and estimated CH_4 emissions from sewer networks using an empirical formula (Supplementary Text S4) [38]. Energy consumption for wastewater transport was calculated based on the usage of pump stations. For the centralized WWTP, data on chemicals, electricity, and effluent quality were obtained from plant records, while GHG emissions (CO_2, CH_4, N_2O) were simulated using the SUMO software. Further, inventory data for plants under SDS scenarios were also simulated using SUMO. Detailed construction and operational inventory data are presented in Supplementary Tables S20–S28.

We accounted for avoided environmental impacts attributable to resource recovery through four displacement credits. (i) We assumed that land application of composted sludge substitutes mineral fertilizers using mineral fertilizer equivalents for nitrogen

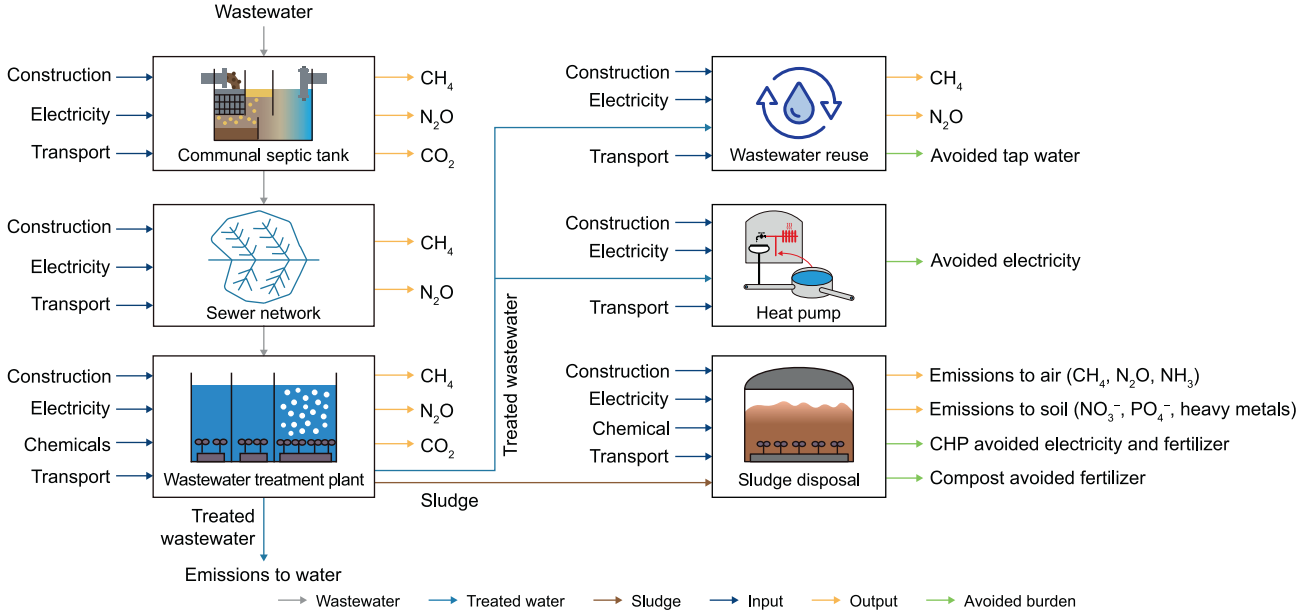

Fig. 3. Life cycle assessment system boundaries for centralized systems (CSs) and scaled decentralized systems (SDSs). CHP, combined heat and power.

and phosphorus (Supplementary Text S5) [39]. (ii) We credited biogas recovery from anaerobic digestion for offsetting electricity demand. (iii) We used HPs to recover thermal energy, replacing electricity demand for heating and air conditioning [40]. (iv) We assumed WR substitutes tap water, thus avoiding energy and chemical consumption in its production and transportation [41].

2.4.3. Life cycle assessment and interpretation

Environmental impacts were evaluated using the ReCiPe 2016 Midpoint (H) and Endpoint (H) methods, which are widely adopted in water system LCA studies due to their comprehensive impact assessment capabilities [42]. The midpoint analysis focused on six key impact categories: fossil resource scarcity (FFP), freshwater ecotoxicity (FETP), freshwater eutrophication (FEP), global warming potential (GWP), human carcinogenic toxicity (HTPc), and terrestrial acidification (TAP) [30,42]. The endpoint assessment incorporated all 18 midpoint categories required by ReCiPe 2016 to evaluate overall damage to human health, ecosystems, and resource scarcity. Environmental impacts were calculated using open LCA software, with the Ecoinvent v3.6 Cutoff database serving as the primary data source. The exact process names for construction and operational inputs, as well as emissions, are presented in Supplementary Tables S29 and S30.

2.4.4. Uncertainty analysis

To enhance computational efficiency, uncertainty was managed using a Monte Carlo simulation combined with Latin hypercube sampling. All life cycle inventory (LCI) input and output data were based on baseline values, with each parameter assigned a probability distribution to account for variability. Most parameters followed normal distributions, with defined variation coefficients. However, a few parameters were modeled using triangular distributions [20]. Crystal Ball software performed 10,000 iterations to analyze impact category distributions and provide insights into the uncertainty of LCI contributors. Complete probability distributions and variation coefficients for each parameter are detailed in Supplementary Table S31.

2.4.5. Sensitivity analysis

Monte Carlo sampling was used for sensitivity analysis to identify key drivers via variance contributions and rank-correlation coefficients [43]. In a separate scenario analysis, three main aspects were evaluated: (i) influent characteristics, with ±20% variation in the empirically derived *k*-values (Supplementary Table S32), (ii) the role of communal septic tanks by comparing scenarios with and without their inclusion (Supplementary Table S33), and (iii) future power system structures under IEA projections for 2030 and 2050 (Supplementary Table S34) [44]. Critically, within this assessment of future energy scenarios, combined HP and WR (HP + WR) configurations—derived from foundational scenarios—were specifically evaluated for relevant SDS scales. This aimed to assess synergy and future adaptability by comparing them against environmentally corresponding single-recovery options (WR or HP).

2.5. Life cycle cost analysis

Life cycle cost analysis (LCCA) quantitatively assesses the long-term economic costs of wastewater treatment systems, categorizing investment, operation, maintenance, and replacement costs into capital expenditure (CAPEX) and operational expenditure (OPEX) [45]. LCCA boundaries align with those of the LCA (Section 2.4.1).

CAPEX includes initial system investments, excluding land acquisition. Construction costs for WWTPs were extracted directly from the budget sections of the corresponding engineering design reports (Section 2.4.2). Costs for the sewer network and other components were calculated by applying the unit costs listed in Supplementary Table S35 to their respective material quantities. OPEX includes energy consumption, chemicals, equipment repairs, maintenance, replacement, and labor, with unit costs based on 2022–2024 market averages (Supplementary Table S35). Given the relative stability of construction and operational costs in China during these periods, no inflation adjustment was applied.

The discounted OPEX over the project lifetime is calculated using equation (2), and the total cost (TC) is calculated using equation (3):

$$O = \sum_{t=1}^{\mathrm{T}} \frac{O_t}{(1+\mathrm{r})^t} \tag{2}$$

$$TC = C_{\mathrm{a}} + \sum_{t=1}^{\mathrm{T}} \frac{O_t}{(1+\mathrm{r})^t} \tag{3}$$

Where O is the discounted OPEX over the project lifetime, O_t is the OPEX at time t, r is the discount rate (5%), and T is the time horizon (50 years), and C_{a} is the CAPEX [46]. All costs are positive; benefits—such as energy recovery, chemical savings, and fertilizer substitution—are negative [47]. This LCCA evaluates construction and operational costs for centralized systems and SDSs. The results are presented as cost per functional unit for a comprehensive economic and environmental comparison.

3. Results

3.1. Midpoint environmental hotspots: system performance comparison and design drivers

This section presents the comprehensive midpoint LCA results for 29 wastewater treatment scenarios, evaluating six key environmental indicators: FFP, FETP, FEP, GWP, HTPc, and TAP. The analysis highlights distinct performance patterns and the decisive influence of system design choices within this specific urban case study.

Environmental impacts varied substantially across scenarios (Fig. 4 and Supplementary Fig. S5). CS-BAU generally revealed higher impacts across all indicators (e.g., 25th for FFP at 0.231 kg oil-eq m^{-3} and 23rd for GWP at 2.189 kg CO_2-eq m^{-3}). Upgrading with energy recovery and WR (CS-CHP + WR) improved performance, thereby reducing FFP by 69% and GWP by 37% and achieving the lowest FETP value at 0.007 kg 1,4-dichlorobenzene equivalents (1,4-DCB-eq) m^{-3}. Overall, the SDS20-MBBR-WR configuration performed the most favorably in this case study, with comparatively 2.7–60.5% lower values across five of six indicators (except FETP) when compared to the CS-CHP + WR scenario (Supplementary Table S36). These performance differences are influenced by key design factors, including WWTP scale, core technology, and resource recovery strategy.

The life cycle contribution analysis across representative scenarios reveals stage-specific impact patterns (Fig. 5). For FFP, FETP, FEP, HTPc, and TAP, operational phases—particularly WWTP operation—dominate the totals (32.1–93.9%; Fig. 5 and Supplementary Fig. S6). Construction burdens are comparatively minor (2.8–52.4%), mainly from sewer networks (0.8–8.0%) and WWTP (0.8–43.1%), while CW systems show higher construction shares (>10%) for most indicators except FEP. In contrast, GWP exhibits a distinct structure driven primarily by upstream communal septic tank CH_4 emissions, which contribute 24.4–46.8% of life-cycle GWP (orange segments in Fig. 5d and

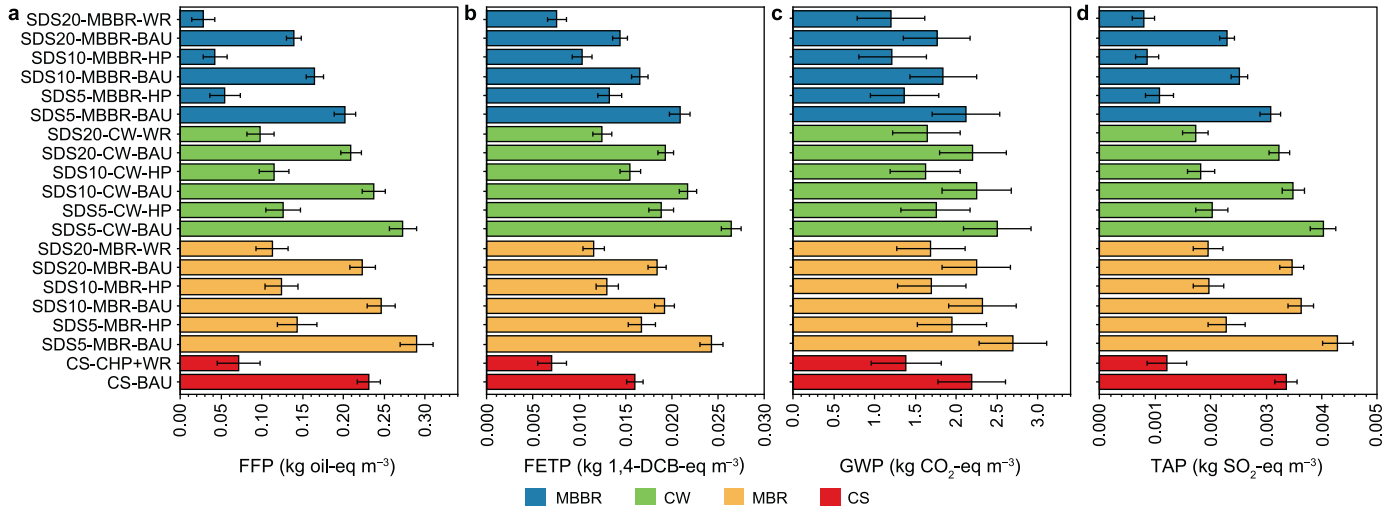

Fig. 4. Midpoint life-cycle impacts across centralized and scaled decentralized scenarios. Midpoint impacts—fossil resource scarcity (FFP, **a**), freshwater ecotoxicity (FETP, **b**), global warming potential (GWP, **c**), and terrestrial acidification (TAP, **d**)— are shown for the centralized system (CS) and the scaled decentralized system (SDS) scenarios using constructed wetland (CW), membrane bioreactor (MBR), and moving bed biofilm reactors (MBBR) technologies. Results are reported for three SDS scales: SDS5 (each plant with a capacity of 5000 m^3 d^{-1}, 20 facilities), SDS10 (each plant with a capacity of 10,000 m^3 d^{-1}, 10 facilities), and SDS20 (each plant with a capacity of 20,000 m^3 d^{-1}, 5 facilities). For SDS technology–scale combinations, bars represent the midpoint impact of the baseline (business-as-usual, BAU) and the best-performing resource-recovery configuration, including water reuse (WR) and heat pump (HP) recovery. For the CS, results include combined heat and power with water reuse (CS-CHP + WR). FETP is expressed as 1,4-dichlorobenzene equivalents (1,4-DCB-eq).

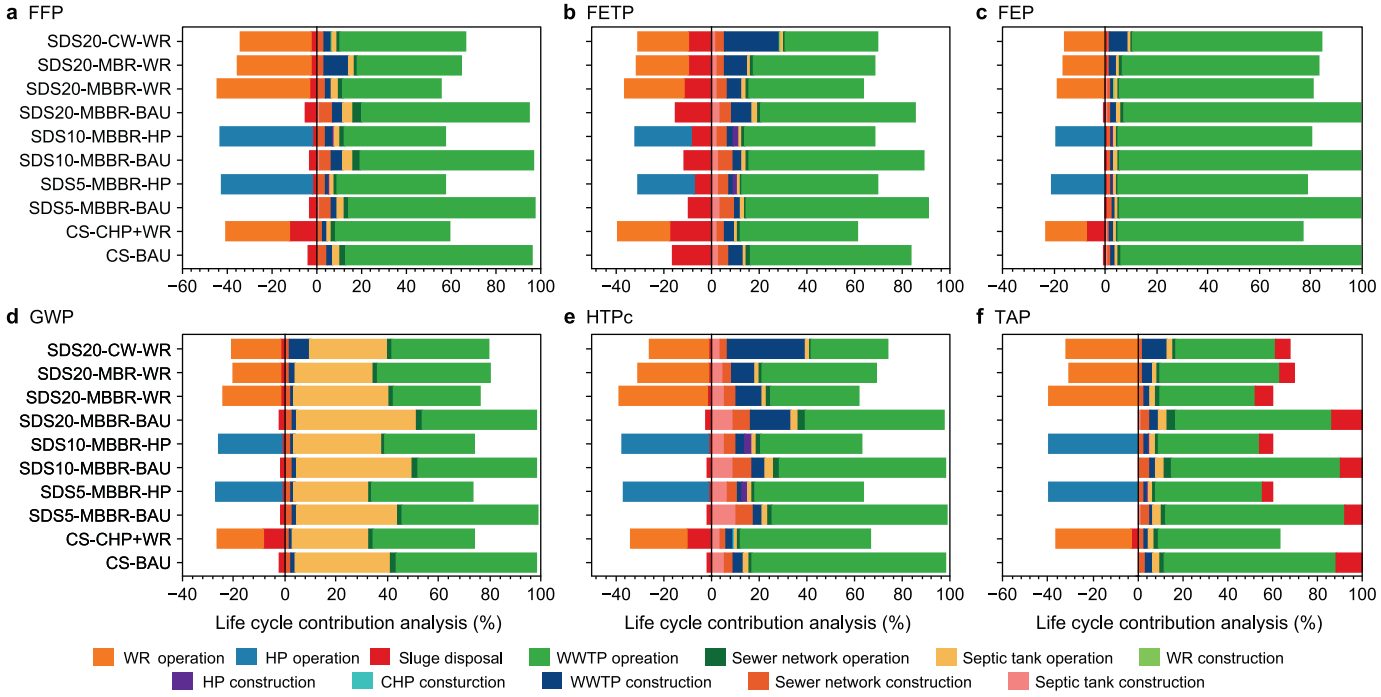

Fig. 5. Life cycle contribution analysis for six midpoint indicators across representative scenarios. a, Fossil resource scarcity (FFP). **b**, Freshwater ecotoxicity (FETP). **c**, Freshwater eutrophication (FEP). **d**, Global warming potential (GWP). **e**, Human carcinogenic toxicity (HTPc). **f**, Terrestrial acidification (TAP). Contributions of key life-cycle phases are shown for the centralized system (CS) and scaled decentralized system (SDS) scenarios, including CS under business-as-usual (BAU) and combined heat and power with water reuse (CHP + WR), and SDS configurations at three scales shown as BAU and the best-performing recovery option. For SDSs, scenarios are primarily based on moving bed biofilm reactor (MBBR) technology, with additional comparisons for SDS20-MBR-WR and SDS20-CW-WR. Complete results are provided in Supplementary Fig. S6. Definitions: SDS5 (each plant with a capacity of 5000 m^3 d^{-1}, 20 facilities); SDS10 (each plant with a capacity of 10,000 m^3 d^{-1}, 10 facilities); SDS20 (each plant with a capacity of 20,000 m^3 d^{-1}, 5 facilities). MBR, membrane bioreactor; CW, constructed wetland; WR, water reuse; HP, heat pump. WWTP, wastewater treatment plant.

Supplementary Fig. S6), often comparable to or exceeding WWTP operational contributions. Further, resource and energy-recovery measures (WR, CHP, and HP) consistently deliver avoided-burden credits (shown as negative contributions) that effectively offset net impacts across all indicators.

These contribution patterns correspond to distinct process-level drivers, which are further examined through a variance-based sensitivity analysis (Supplementary Table S37). Electricity consumption in WWTP operations was the dominant driver for FFP, HTPc, and TAP (>78.4% of the variance). GWP variance was

overwhelmingly determined by CH_4 emissions from communal septic tanks (90.7–97.2%), with WWTP electricity accounting for only 1.4–6.0%. FETP variance was predominantly driven by WWTP electricity (32.7–78.9%), followed by the ecotoxicity burden associated with $FeCl_2$ used for phosphorus removal (13–53.4%). FEP was primarily driven by effluent TP discharge (82.8–97.7%), with electricity as a secondary driver. These findings emphasize the need to optimize energy and chemical use throughout the system's life cycle, which in turn is influenced by broader design choices.

Indeed, the WWTP scale exhibits clear environmental benefits tied to increased scale. Higher-capacity SDS configurations (SDS5–SDS20) generally reduced impacts across all six midpoint indicators (Fig. 4 and Supplementary Fig. S5). This benefit primarily stems from enhanced operational efficiency and scale economies in larger WWTPs, leading to lower energy consumption intensity and more efficient material use [48]. For example, when the WWTP scale increased from SDS5 to SDS20, the energy consumption intensity decreased by 32.7% in MBBR, 21.3% in MBR, and 25.4% in CW systems. This efficiency gain translated into reductions ranging from 15.1% to 31.1% in energy-intensive impacts (FFP, FETP, HTPc, and TAP) (Supplementary Table S38). GWP reductions were more modest (12.0–16.9%) because upstream communal septic tank CH_4 emissions remain constant per unit of treated wastewater. Consequently, as plant-side burdens decline through scale optimization, the relative contribution of these upstream emissions increases from 39.5% in SDS5-MBBR-BAU to 46.8% in SDS20-MBBR-BAU (Fig. 5d). In the SDS20-MBBR-BAU scenario, almost half of the GWP (0.86 out of 1.76 kg CO_2-eq m^{-3}) originated from these upstream sources, which is comparable to the 0.82 kg CO_2-eq m^{-3} from plant operations.

The selection of core technology exerted a more substantial impact. MBBR, particularly in SDS20-MBBR-WR, was favorable under the studied context, thus revealing all the lowest impacts; the only exception was in FETP, which was related to $FeCl_2$ dosing for phosphorus removal. This superiority is attributed to MBBR's biofilm, which reduces aeration requirements, thereby leading to significantly lower specific energy consumption intensity (0.35 kWh m^{-3} for an SDS20 plant), approximately 45% less than MBR under equivalent conditions. CW configurations with AMBR pre-treatment had high HTPc impacts (contribution of 24.3–43.1%) from construction material intensity (Fig. 5 and Supplementary Fig. S6), thus partially offsetting their moderate operational energy advantages [49].

Further, integrating resource recovery strategy (HP or WR) consistently improved all six indicators by reducing net energy use and resource demand (Fig. 4). Avoided electricity emerged as a major mitigating factor in both HP (Supplementary Table S39) and WR (Supplementary Table S40) scenarios and accounted for 20.2–52.8% of variance reduction in energy-related impacts (FFP, FETP, HTPc, and TAP). Recovery technology effectiveness proved scale-dependent: HP yielded greater benefits at more distributed configurations (SDS5 and SDS10) through efficient thermal energy recovery over shorter supply distances [50], although this advantage diminished at the SDS20 scale as heat distribution losses became more pronounced. In contrast, under the conditions evaluated in this study, WR had a clear advantage: benefits from avoided freshwater abstraction and transport [51]—likely less affected by scale-dependent distribution losses than HP—outweighed the latter's reduced efficiency, thus solidifying SDS20-MBBR-WR's top overall rank.

Upstream communal septic tanks are a persistent GHG hotspot that may substantially constrain the achievable reduction in GWP in wastewater systems, even when downstream processes are optimized. Although the assumed regional CH_4 emission rate (7.88 g CH_4 per capita per day) is below the default values reported by the Intergovernmental Panel on Climate Change [52], these units still account for 24.4–46.8% of total life-cycle GWP across all evaluated scenarios. This large and relatively invariant contribution highlights the need for mitigation strategies that extend beyond WWTP boundaries, including the consideration of removing the communal septic tank.

3.2. Endpoint damage assessment results

Endpoint assessment quantified midpoint impacts across three primary areas of protection (AoPs): human health, ecosystems, and resource scarcity. Consistent with the midpoint findings presented in Section 3.1, SDS configurations exhibited economies of scale, as endpoint damage decreased proportionally with increasing scale (SDS5 to SDS20) across all AoPs.

In configurations without resource recovery, MBBR-based SDS generally incurred lower endpoint damages than the CS-BAU scenario across all AoPs and scales (Fig. 6a–c). MBR configuration presents moderate damage, and even less for larger scales. In contrast, CW configurations experienced endpoint damage comparable to or exceeding CS-BAU; construction materials were major contributors [37], particularly to resource scarcity at larger scales.

Integrating resource recovery reduced endpoint damage by 30.1–62.6% across all evaluated configurations and AoPs. As presented in Section 3.1, SDS20 configurations performed best with WR, SDS5, and SDS10 with HP recovery, while the CS configuration favored a CHP + WR approach, thus leveraging the benefits of centralized sludge treatment. Accordingly, only the most advantageous recovery option for each scale is presented (Fig. 6d–f). The SDS20-MBBR-WR scenario achieved the minimum damage potentials for human health (3.1×10^{-6} disability-adjusted life years [DALYs] m^{-3}), ecosystems (1×10^{-8} species·yr m^{-3}), and resource scarcity (6.8×10^{-3} USD m^{-3}), which constituted half of this scenario's BAU. In comparison, the SDS20-MBR-WR scenario incurred higher damage, with its membrane-related energy consumption being 80% higher than that of SDS20-MBBR-WR. The CW scenario's endpoint damages were amplified by its construction footprint, particularly due to resource scarcity. The CS-CHP + WR also failed to demonstrate an advantage, with energy contributing 28.9–34.4% and chemicals contributing 12.4–27.0% to total impacts.

The assessment identified significant contributions from distinct lifecycle inputs and phases. Specifically, upstream communal septic tank CH_4 emissions contributed 9.2–12.2% to climate change-related damages (e.g., 1.08×10^{-6} DALY m^{-3} for human health and 3.43×10^{-9} species·yr m^{-3} for ecosystems). Construction materials accounted for up to 23.8% of resource scarcity damages, with sewer networks constituting over half of this share. Operational trade-offs were also evident: for example, the use of $FeCl_2$ for phosphorus removal provided a 1.3% FEP-related benefit to the ecosystem. However, it also incurred an 8.0% drawback to the same AoP via other pathways (e.g., upstream chemical production and energy-related emissions) and a 4.7% detriment to resource scarcity. In sludge management, resource recovery reduced resource scarcity damage (by 7.7×10^{-3} USD m^{-3}) and ecosystem damage (by 5.6×10^{-9} species·yr m^{-3}), while residual contaminants added 9.1×10^{-7} DALYs m^{-3} to human health damage.

3.3. Economic optimality: LCC insights for SDS

The LCC analysis of the 29 evaluated scenarios revealed total costs ranging from 0.40 to 1.12 CNY m^{-3} (Fig. 7). For the CS

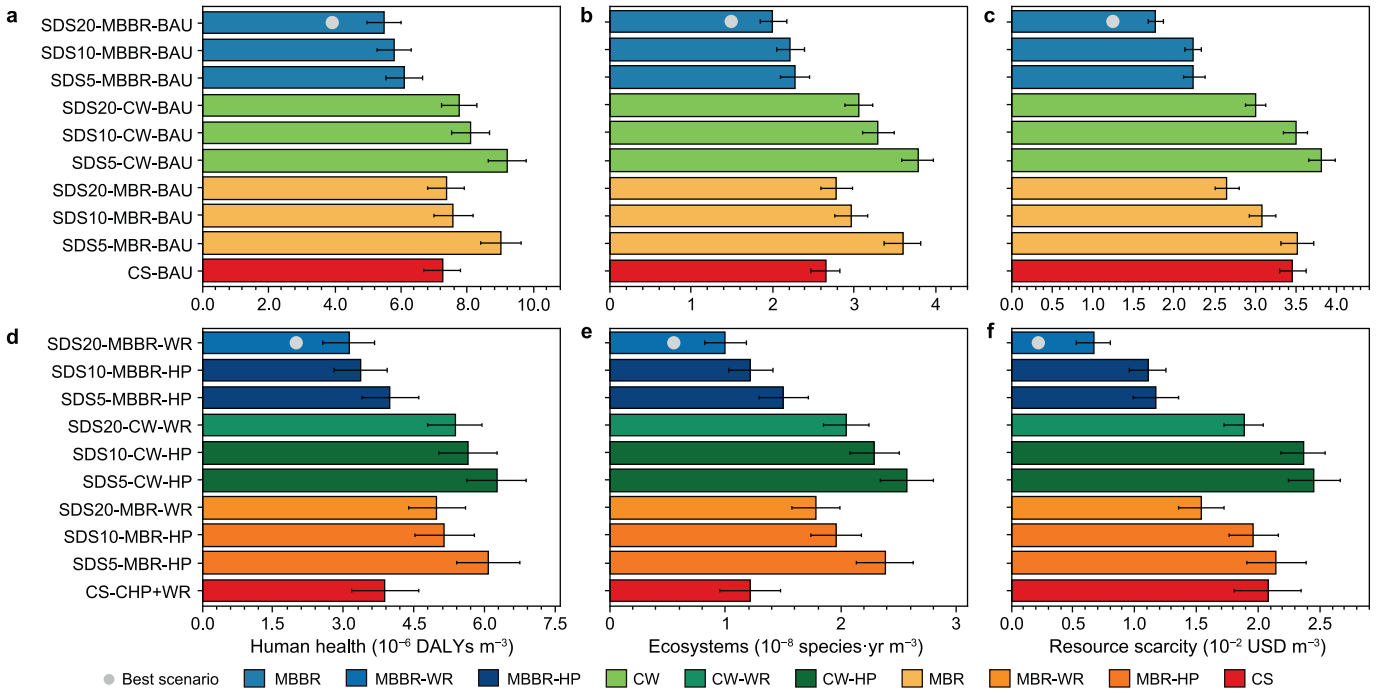

Fig. 6. Endpoint life-cycle impacts for centralized systems (CSs) and scaled decentralized systems (SDSs) scenarios, with and without resource recovery. a–c, Baseline scenarios without resource recovery (business-as-usual, BAU): human health damage (disability-adjusted life years, DALYs), ecosystem damage (species·yr), and resource scarcity (USD). **d–f**, Scenarios with resource recovery, including CS with combined heat and power with water reuse (CS-CHP + WR) and SDS configurations with resource recovery. For SDSs, results are presented for three scales—SDS5 (each plant with a capacity of 5000 m^3 d^{-1}, 20 facilities), SDS10 (each plant with a capacity of 10,000 m^3 d^{-1}, 10 facilities), and SDS20 (each plant with a capacity of 20,000 m^3 d^{-1}, 5 facilities)—and for three treatment technologies: moving bed biofilm reactor (MBBR), membrane bioreactor (MBR), and constructed wetland (CW). For each technology–scale combination, bars represent the endpoint impact of the best-performing resource-recovery option, including water reuse (WR) and heat pump (HP) recovery. The overall optimal scenario, with the lowest aggregate endpoint impact among those shown, is highlighted by a gray circle.

configuration, integrating resource recovery reduced the LCC by 16.9%, from 0.59 CNY m^{-3} (CS-BAU) to 0.49 CNY m^{-3} (CS-CHP + WR), thus demonstrating the economic viability of energy and water reuse in large-scale infrastructures.

Within SDSs, LCC generally decreased with increasing system scale; however, it varied widely across core technologies. CW configurations had the highest LCC across all scenarios, with construction capital expenditures accounting for 51.0–62.0% of the total LCC. MBR configurations ranked second-highest in LCC, primarily due to operational costs for membrane replacement (every five years, 10.7% of LCC) and membrane fouling mitigation [53]. MBBR configurations at the SDS20 scale consistently had lower LCCs than CS-CHP + WR. Among them, the SDS20-MBBR-WR scenario achieved the lowest LCC among all evaluated configurations (0.40 CNY m^{-3}) due to low energy consumption intensity, durable biofilm media [54], and effective WR offsetting freshwater needs. Aligned with its minimal environmental impact, this dual optimality in LCC and LCA positions SDS20-MBBR-WR as a highly promising strategy within the context of this study.

Comparing resource recovery options within SDSs, HP configurations consistently exhibited higher LCCs than WR scenarios at equivalent scales. This economic disadvantage stems from their higher capital costs, primarily driven by the substantial investment required to connect heat distribution pipelines to urban demand [55]. This finding reveals an initial economic challenge for HP integration, particularly when viewed against its environmental benefits at smaller SDS scales (SDS5 and SDS10).

3.4. Synergistic gains via combined resource and energy recovery

Building on the promising economic and environmental performance of SDS20-MBBR-WR, this section evaluates the enhanced performance achieved by integrating HP to create a combined resource recovery strategy (SDS20-MBBR-WR + HP) for comparison (Fig. 8).

The combined SDS20-MBBR-WR + HP strategy yielded substantial environmental benefits across midpoint indicators (Fig. 8a–e). For the critical GWP, the strategy achieved 0.66 kg CO_2-eq m^{-3}, approximately 45% lower than the SDS20-MBBR-WR scenario (1.20 kg CO_2-eq m^{-3}) and 52.5% lower than CS-CHP + WR (1.39 kg CO_2-eq m^{-3}). It also transformed burdens into net benefits for FFP, HTPc, and TAP, with further improvements in FEP and FETP (Supplementary Table S41). These gains extended to endpoint assessments (Fig. 8f–h), with 74.1% lower human health damage and net resource benefits (-3.0×10^{-3} USD m^{-3}) versus SDS20-MBBR-WR. SDS20-MBBR-WR + HP outperformed CS-CHP + WR across all AoPs, while maintaining a lower LCC at 0.37 CNY m^{-3}—which is more cost-effective than CS-CHP + WR (0.49 CNY m^{-3}) and SDS20-MBBR-WR (0.40 CNY m^{-3}) (Fig. 8i). This indicates that the significant environmental enhancements were achieved without compromising economic viability, thereby reflecting a highly advantageous performance profile for the combined strategy within the context of this study.

4. Discussion

4.1. Performance drivers and design trade-offs across the treatment chain

4.1.1. Upstream impacts: influent quality and conveyance system performance

This study employed a field-calibrated first-order kinetic model to characterize how shorter sewer networks in SDSs alter WWTP influent quality by limiting in-sewer transformations (detailed in

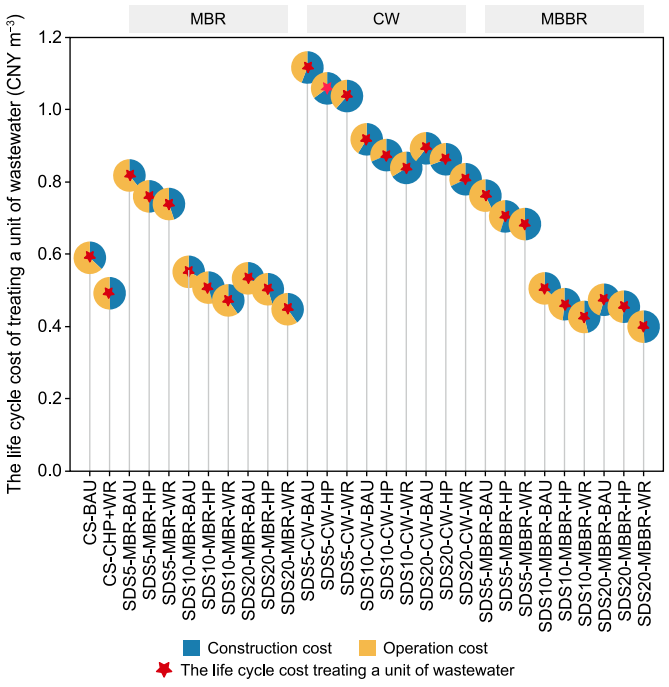

Fig. 7. Life cycle cost (LCC) analysis of centralized systems (CSs) and scaled decentralized systems (SDSs). Total LCC includes construction and operation costs for the CS and SDS configurations using membrane bioreactor (MBR), constructed wetland (CW), and moving bed biofilm reactor (MBBR) technologies. Scenarios include business-as-usual (BAU) for both systems, combined heat and power with water reuse (CHP + WR) for the CS, and water reuse (WR) and heat pump (HP) recovery for the SDSs. Results are shown for three SDS scales: SDS5 (each plant with a capacity of 5000 m^3 d^{-1}, 20 facilities), SDS10 (each plant with a capacity of 10,000 m^3 d^{-1}, 10 facilities), and SDS20 (each plant with a capacity of 20,000 m^3 d^{-1}, 5 facilities).

Supplementary Texts S1 and S2). Reduced conveyance distances constrain COD degradation during transport, thus preserving higher COD concentrations at WWTP inlets and increasing COD/TN ratios by 17.1% from CS (8.2) to SDS5 (9.6). This elevation reduces or eliminates the need for external carbon supplementation: the CS-BAU plant requires methanol addition (38.7 g m^{-3}) to compensate for in-sewer carbon depletion and achieve Class A nitrogen removal standards, whereas all SDS configurations achieve these standards without supplemental carbon, thus benefiting from both more favorable influent quality and optimized process configurations. However, shorter conveyance also reduced TP removal via sedimentation (CS: 7.3 mg L^{-1} vs. SDS5: 7.9 mg L^{-1}), thereby increasing downstream chemical demands. This effect was particularly pronounced in MBBR systems [56], which primarily rely on chemical precipitation for phosphorus removal: $FeCl_2$ dosing increased by 50% from SDS20 to SDS5. These shifts indicate the need to customize process design to SDS-specific influent profiles and, thus, strike a balance between the benefits of elevated COD/TN ratios and the increased TP removal requirements for optimal environmental outcomes.

A ±20% sensitivity analysis on *k* values confirmed robustness while revealing technology-specific responses. Most midpoint indicators (e.g., FFP, FETP, FEP, HTPc, and TAP) and all endpoint indicators fluctuated minimally (<1%), thereby affirming the model's LCA applicability. However, GWP displayed higher sensitivity, particularly in MBR systems (up to 20.2% vs. <8.6% in other technologies; Supplementary Tables S42 and S43), primarily driven by N_2O emissions rather than energy consumption. A ±20% change in *k* values resulted in N_2O-related GWP variations of approximately 21% in MBR systems, significantly higher than in other technologies, while energy-related GWP impacts varied by only 2–3% across all configurations. This reflects MBR's tighter process control and higher nitrification intensity, both of which amplify N_2O production from fluctuations in the influent COD/TN ratio during denitrification [57].

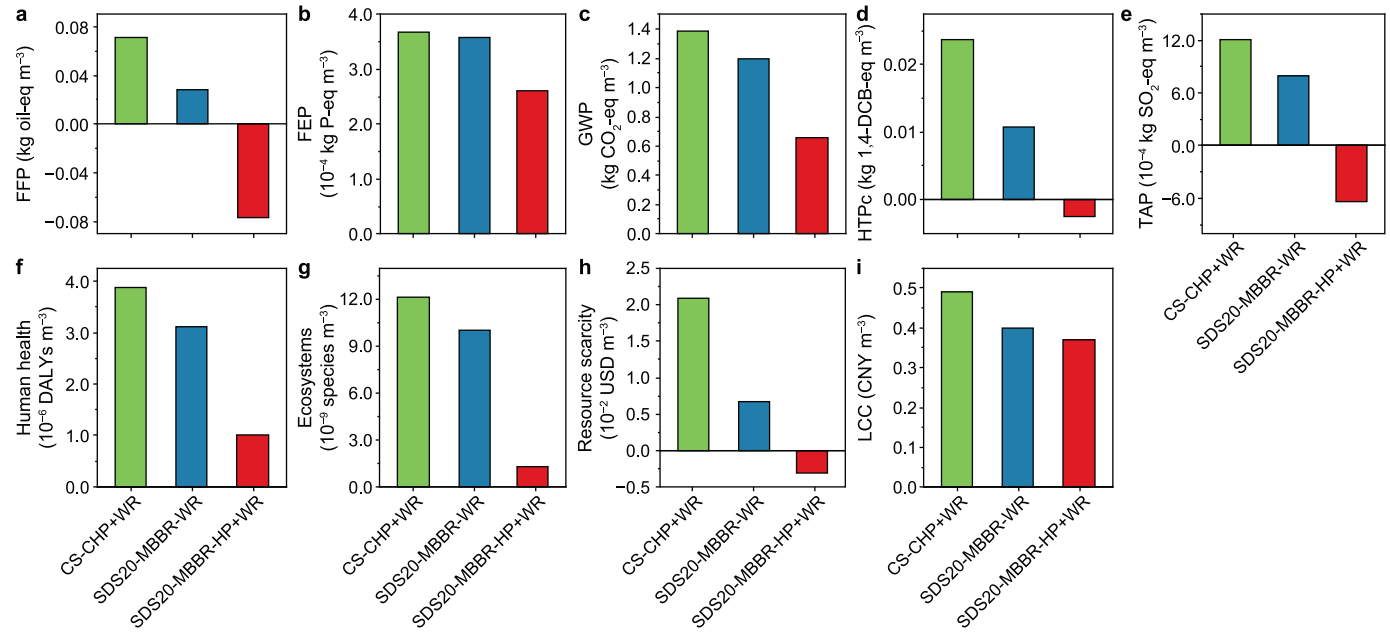

Fig. 8. Midpoint and endpoint life-cycle impacts and economic performance across key wastewater treatment scenarios. Centralized system with combined heat and power with water reuse (CS-CHP + WR) and scaled decentralized systems with a plant capacity of 20,000 m^3 d^{-1} (SDS20) using a moving bed biofilm reactor (MBBR) with water reuse (WR) and a MBBR with heat pump and water reuse (HP + WR) are compared. **a**–**e**, Midpoint indicators: fossil resource scarcity (FFP, **a**), freshwater eutrophication (FEP, **b**), global warming potential (GWP, **c**), human carcinogenic toxicity (HTPc, **d**), and terrestrial acidification (TAP, **e**). **f**–**i**, Endpoint damage categories: human health (**f**), ecosystems (**g**), resource scarcity (**h**), and life cycle cost (LCC, **i**). HTPc is expressed as 1,4-dichlorobenzene equivalents (1,4-DCB-eq).

4.1.2. Core treatment technologies: balancing constraints and performance

Optimal SDS design in high-density urban areas with stringent discharge standards necessitates balancing construction impacts with operational demands, thereby requiring prioritizing robust, compact, and performance-based technologies. Among those evaluated, MBBR is highly suitable due to its low energy demand, small spatial footprint, long carrier lifespan [54], and strong adaptability to influent variations, thereby ensuring stability and providing flexibility for phased construction and urban integration [58]. However, its notable reliance on chemical dosing for phosphorus removal presents a key trade-off. MBR also provides high effluent quality and a small carbon footprint, but demands careful energy management and membrane maintenance (five-year replacement cycles) [53]. Conversely, CWs—despite ecological benefits and low operational energy—face significant restrictions due to their large footprint (e.g., reactor volumes 173–245% larger than MBR and MBBR systems), high construction impacts, and substantial lifecycle costs, thereby limiting their applicability in urban or high-density settings [31,37]. To consistently achieve Class A standards, all three technologies benefit from integration with anoxic or anaerobic stages for effective nitrogen removal. Ultimately, effective selection of core SDS technologies requires a holistic approach that balances land availability, capital investment, operational burdens, and specific pollutant-removal needs for sustainable deployment in dense urban contexts.

4.1.3. Downstream strategies: integrated resource recovery

Traditional large WWTPs, following a “treat-and-discharge” pattern, often constrain efficient resource recovery due to their distance from urban centers despite scale economies [59]. In contrast, SDSs, being closer to demand centers, significantly enhance the feasibility and efficiency of localized recovery, although their efficacy varies with scale.

WR is crucial for sustainable urban water management—particularly in water-scarce regions—supporting urban greening, ecological replenishment, and industrial cooling, thereby avoiding the burdens of long-distance freshwater delivery—a benefit more pronounced in SDSs [51]. However, in China, reuse remains mainly non-potable due to limited public acceptance (e.g., only 8.4% strong acceptance in Beijing [60]), regulatory restrictions, and the presence of emerging contaminants. Integrating heat recovery (HP) provides a complementary pathway. Proximity enables low-grade thermal energy extraction from treated effluents, with efficient transport feasible only within 3–5 km due to heat losses [61]. Thus, smaller SDSs (e.g., SDS5 and SDS10) can directly leverage HPs for local heating or cooling. While HP's standalone economic viability is often constrained by high lifecycle costs of distribution pipelines [55], its integration into combined resource recovery strategies (WR + HP) can achieve significant overall cost reductions through synergies.

4.2. The communal septic tank demolition dilemma: system-wide environmental trade-offs

Communal septic tanks were retained in baseline scenarios as they remain embedded in existing Chinese urban infrastructure, despite new installations being prohibited under GB 50014-2021. Section 3.1 identified CH_4 emissions from these septic tanks as contributing 24.4–46.8% of total GWP and accounting for over 89.3% of the uncertainty. While providing preliminary reductions in COD, NH_4^+-N, and TP, the disproportionate GHG burden of communal septic tanks has prompted discussions about removal [15]. However, evaluating septic tank removal requires understanding system-wide trade-offs beyond isolated emission reductions.

In this study, influent COD concentrations to the WWTP increased by approximately 20.5% (from 442.5 to 532.8 mg L^{-1}) in the CS-BAU scenario when the communal septic tank is removed (Supplementary Table S33), a finding comparable to investigations in Chongqing [62]. Increased influent COD particularly benefits WWTPs that initially face low COD/TN ratios and require external carbon addition [63]. For the CS-BAU plant, septic tank removal is expected to reduce methanol supplementation by approximately 10%, thereby lowering associated operational costs and GHG emissions. However, the concurrent rise in TP concentrations increases the demand for phosphorus removal chemicals and their associated emissions. This effect is particularly noticeable in SDS, such as the SDS5 MBBR plant, where GHG emissions from TP removal increased by 13.3%.

From a life-cycle GHG perspective, the elimination of direct septic tank CH_4 emissions yields substantial net reductions (24.3–68.6%) across diverse CS and SDS configurations, both without resource recovery and under optimal recovery conditions (Fig. 9a). The SDS20-MBBR-WR scenario revealed the largest decrease (68.6%), primarily because communal septic tank CH_4 emissions constituted a large proportion (37.2%) of this configuration's total life cycle GHG footprint, which is in contrast with its relatively efficient operational phase. However, this benefit is partially offset by burden shifting—removing communal septic tanks increases the COD entering sewer networks, correspondingly elevating CH_4 emissions across all network scales by approximately 20% (Supplementary Table S44), as in-sewer methane production is positively correlated with COD under constant hydraulic conditions [64,65]. Additionally, increased solids loading introduces sedimentation risks that require adapted infrastructure management. The increase in operational GHG emissions at the WWTP reveals a strong technology-dependent pattern (Fig. 9b). Removal of communal septic tanks increases influent COD (by 20.5%) and TN (by 9.3%). The GHG increase is most pronounced in CW systems (12.1–28.8%), moderate in MBR configurations (10.5–16%), and minimal in MBBR and CS systems (2.3–6.7%). This disparity is primarily driven by technology-specific N_2O production under increased loading. CW systems, with their limited DO control via natural aeration [66], are particularly prone to elevated N_2O emissions (which can comprise up to 52.3% of their direct GHGs). In contrast, the precise aeration control in MBBR and CS systems keeps N_2O production low and stable, thereby effectively mitigating the impact of loading variations [33,67].

Overall, while communal septic tank removal consistently improves human health and ecosystem quality across all scenarios (by mitigating high-impact CH_4 emissions), its impact on resource scarcity depends on downstream treatment efficiency. Only centralized systems and MBBR-based SDSs demonstrated net benefits for resource scarcity. Conversely, for MBR and CW configurations, increased operational intensity due to higher loads (particularly greater energy and chemical demand) led to increased resource depletion, thus potentially offsetting the environmental benefits of eliminating communal septic tank CH_4 emissions. This highlights a critical finding: the inherent energy and chemical efficiency of the selected WWTP technology is decisive in determining whether communal septic tank removal achieves overall environmental benefits or merely shifts burdens toward resource depletion.

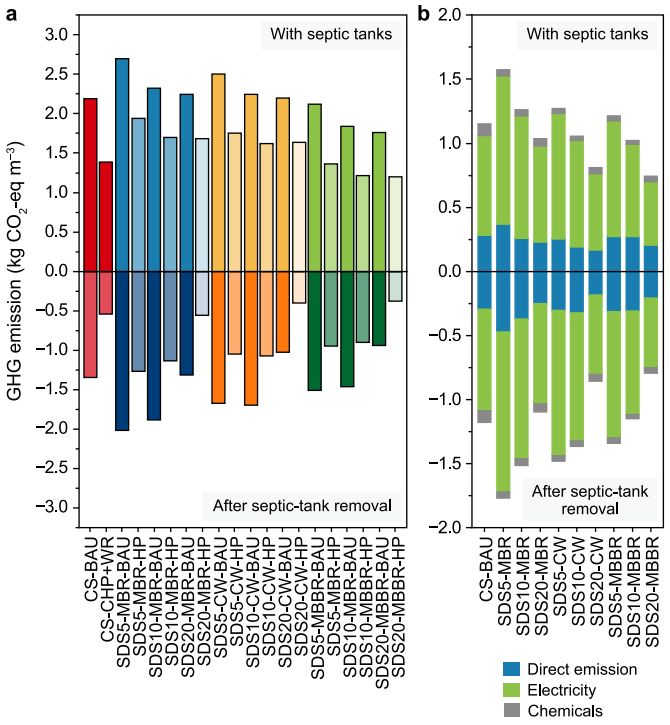

Fig. 9. Greenhouse gas (GHG) emissions before and after removal of communal septic tanks. a, Life-cycle GHG emissions for the centralized system (CS) and the scaled decentralized system (SDS) configurations, shown without resource recovery or with optimal recovery. SDS configurations use membrane bioreactor (MBR), constructed wetland (CW), and moving bed biofilm reactor (MBBR) technologies. Results are shown for three SDS scales: SDS5 (each plant with a capacity of 5000 m^3 d^{-1}, 20 facilities), SDS10 (each plant with a capacity of 10,000 m^3 d^{-1}, 10 facilities), and SDS20 (each plant with a capacity of 20,000 m^3 d^{-1}, 5 facilities). Scenarios include business-as-usual (BAU) for both systems, combined heat and power with water reuse (CHP + WR) for the CS, and water reuse (WR) and heat pump (HP) recovery for the SDSs. **b**, Operational GHG emissions at wastewater treatment plants by scale and technology, including direct emissions (methane, CH_4; nitrous oxide, N_2O; fossil carbon dioxide, fossil CO_2) and indirect emissions associated with electricity and chemical inputs.

4.3. Future-proofing the resource recovery performance of SDSs under evolving energy

To evaluate the long-term performance of these wastewater management schemes under future energy projections, a sensitivity analysis with a focus on representative systems was conducted, including a conventional centralized system (CS-CHP + WR) and various scales (SDS5, SDS10, SDS20) of MBBR-based SDSs with single or combined resource recovery. The analysis considered China's power grid decarbonization trajectory, with non-fossil energy shares projected to reach 44% by 2030 and 77% by 2050 [44] (Supplementary Table S34).

Under the current energy mix, MBBR-based SDSs generally exhibited lower GWP across all scales than in the CS-CHP + WR scenario (Fig. 10a), with SDS10-MBBR-HP + WR and SDS20-MBBR-HP + WR showing the lowest values. However, as the power grid decarbonizes toward 2030 and 2050, absolute GWP for combined recovery (HP + WR) MBBR configurations is projected to increase by approximately 36.9–70.7% relative to 2020 levels. This counterintuitive trend arises because grid decarbonization significantly diminishes the avoided emission benefits from HP and WR, as the substituted electricity becomes less carbon-intensive [68]. Despite this increase in absolute GWP, SDS10-MBBR-HP + WR often retained a relatively optimal GWP position. This sustained performance in future scenarios is attributed to shorter sewer networks that reduce fugitive CH_4 emissions as well as the increasing relative importance of inherent direct biological (N_2O) and upstream (communal septic tank CH_4) emissions as electricity emissions decrease.

For endpoint damage indicators, SDS20-MBBR-HP + WR consistently had the best performance across all timeframes (2020, 2030, and 2050; Fig. 10b–d), thereby demonstrating robust mitigation potential for human health and ecosystem impacts. The evolving energy mix also influenced these endpoint indicators; for example, increased reliance on nuclear and hydropower by 2030 could temporarily increase water consumption, thus impacting human health and ecosystem metrics. Conversely, widespread adoption of solar and wind by 2050 is projected to reduce resource scarcity. Nevertheless, the substantial water demands of nuclear and hydropower remain a key consideration in water-stressed regions. These findings emphasize that no single optimal configuration is universally static; rather, system performance is dynamic and significantly influenced by external factors, such as the evolving energy mix and regional water availability.

4.4. Strategic considerations and implementation pathways for SDSs

LCA and LCCA results for a high-density city in Northern China with stringent Class A standards reveal that SDS integration is a viable pathway for urban wastewater management, but findings remain case-specific and require contextual adaptation.

Strategically, deploying SDSs as urban regional nodes provides significant advantages, inherently reducing capital outlays for new long-distance trunk sewers and substantially reducing conveyance energy [12]. For example, our SDS5 configuration demonstrated an approximate 23% reduction in conveyance energy. SDS implementation adapts to diverse urban contexts: in established areas where centralized reconstruction is infeasible, SDSs are incrementally integrated by directly intercepting and rerouting wastewater from existing sewer networks within designated catchment areas for localized treatment, in a sequence determined by renewal priorities. For new developments, SDSs serve as primary infrastructure, thus eliminating long-distance sewers and accommodating future capacity by deploying additional, self-contained facilities rather than expanding existing plants. This differentiated approach maintains efficiency, compliance, and optimal adaptation to the urban stage.

Second, effective deployment of resource recovery requires an enabling policy framework. Combined strategies (e.g., SDS20-MBBR-WR + HP) have demonstrated significant economic and environmental benefits, but effective deployment requires enabling policy frameworks. Distributed energy trading, policy incentives, and community pilots can accelerate adoption and improve public acceptance. Recent initiatives—such as Beijing's Renewable Energy Substitution Action Plan (2023–2025), which mandates reclaimed water and wastewater-source HPs within 5 km of reclamation plants, and similar programs in Shanghai, Guangdong, and Shaanxi—illustrate how WR and HP can be embedded into urban energy and water planning. Compared with ground-source HPs constrained by declining groundwater levels in Beijing [69] and air-source HPs limited by severe cold in Northeast China [70], wastewater-source HPs leverage stable urban sewage networks to provide reliable thermal energy recovery.

Third, implementing SDS in dense urban areas faces intertwined challenges. Limited land availability makes siting difficult, while the gradual phase-out of communal septic tanks requires downstream sewers and centralized plants to be upgraded to absorb shifting loads. At the institutional level, wastewater responsibilities are divided among water utilities, environmental

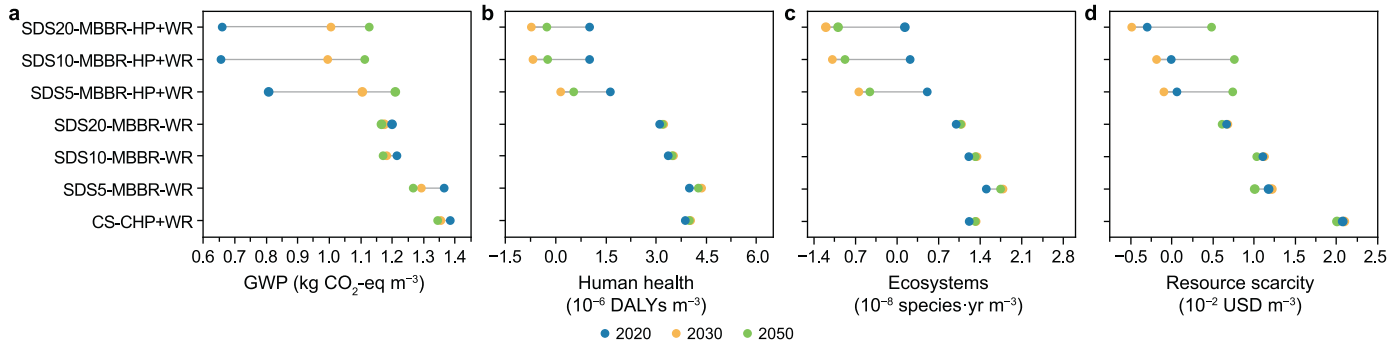

Fig. 10. Environmental impacts of an enhanced centralized recovery scenario versus optimal MBBR-based scaled decentralized systems (SDSs) scenarios under alternative electricity mixes. Centralized system with combined heat and power with water reuse (CS-CHP + WR) and SDS using a moving bed biofilm reactor (MBBR) with water reuse (WR) and a MBBR with heat pump and water reuse (HP + WR) are compared. Results are shown for three SDS scales: SDS5 (each plant with a capacity of 5000 m^3 d^{-1}, 20 facilities), SDS10 (each plant with a capacity of 10,000 m^3 d^{-1}, 10 facilities), and SDS20 (each plant with a capacity of 20,000 m^3 d^{-1}, 5 facilities), under the 2020, 2030, and 2050 energy-mix scenarios: global warming potential (GWP, **a**), human health damage (disability-adjusted life years, DALYs) (**b**), ecosystem damage (**c**), and resource scarcity (**d**).

regulators, and urban planning agencies, resulting in fragmented governance that hampers coordinated action. Addressing these challenges requires integrated planning and gradual infrastructure adjustments, supported by mature, low-complexity technologies such as MBBR, thereby enabling SDSs to be deployed as a practical extension of urban wastewater systems without disrupting overall performance.

4.5. Research limitations and future directions

The current study has several limitations. First, although the empirical first-order kinetic model for pollutant transformation in sewer networks was validated by field data and mechanistic model simulations, it provides only a simplified description of concentration changes and is mainly suitable for LCA inputs, without capturing the mechanistic complexity of in-sewer processes. Second, steady-state SUMO simulations of WWTPs cannot reflect dynamic performance under extreme weather or urban expansion. Third, SDSs in this study are based on conceptual SUMO designs that represent idealized configurations for comparison rather than site-specific implementation.

Future research should incorporate dynamic, long-term simulations that consider population growth, urban redevelopment, and climate change to capture evolving influent characteristics and assess the adaptability of SDS configurations and treatment technologies. Advanced sewer water quality transformation models could be applied to better characterize in-sewer processes and their impacts on system performance. In addition, innovative treatment processes and diversified resource recovery pathways could be evaluated to provide further insights into the long-term sustainability and adaptability of SDSs.

5. Conclusion

This study provided the integrated LCA and LCCA analysis of SDSs in high-density Chinese cities, where communal septic tanks remained embedded as preliminary treatment within sewer networks and downstream centralized plants complied with stringent Class A discharge standards. Our comprehensive evaluation of 29 scenarios, comprising centralized systems and 27 SDS configurations, clearly demonstrated that SDSs provided substantial sustainability advantages through optimized scale, technology selection, and resource recovery.

Further, SDS performance exhibited economies of scale, with 20,000 m^3 d^{-1} configurations generally outperforming smaller scales. Crucially, shorter conveyance distances reduced transport energy but altered influent quality (e.g., increasing COD/TN ratios yet limiting phosphorus removal), thereby necessitating adaptive strategies—such as increased chemical dosing—for compliance. Among the technologies, MBBR achieved the best overall balance, thanks to its low energy demand, despite requiring additional chemicals for phosphorus removal. MBRs provided reliable effluent quality and a small spatial footprint but incurred higher energy costs. Further, despite their ecological benefits, CWs faced significant land constraints, high construction footprints, and substantial lifecycle costs in dense areas. Resource recovery benefits varied with SDS scale, with SDS20-MBBR-WR achieving optimal performance (0.40 CNY m^{-3}). Combined WR + HP integration further enhanced sustainability beyond centralized systems.

Successful SDS implementation hinged on understanding whole-system trade-offs. Communal septic tanks, identified as major GHG hotspots (contributing 24.4–46.8% of total GWP), presented a dilemma: their removal reduced GHG emissions but simultaneously increased downstream pollutant loads, thus requiring robust treatment to prevent burden shifting. Thus, technology selection needed to balance performance with construction and operational burdens. Under future energy transition scenarios, 10,000 m^3 d^{-1} MBBR-HP + WR systems achieved optimal climate performance, while 20,000 m^3 d^{-1} configurations delivered superior human health and ecosystem benefits, thus indicating that optimal configurations vary by impact category. Deployment strategies must be context-specific: in established areas, SDSs should be incrementally integrated into existing networks for localized treatment; in new developments, they can serve as primary infrastructure, thereby eliminating long-distance trunk sewers and achieving localized treatment from the outset. Effective resource recovery through WR and HP technologies required supportive policy frameworks and targeted incentives. Therefore, strategic siting combined with policy alignment was critical for establishing SDSs as foundational infrastructure in sustainable urban systems.

CRediT authorship contribution statement

Aliya Abulimiti: Writing - Original Draft, Visualization, Software, Methodology, Data Curation, Conceptualization. **Boxuan Wang:** Writing - Review & Editing, Data Curation, Visualization. **Xiuheng Wang:** Writing - Review & Editing, Supervision, Methodology, Investigation, Funding Acquisition, Conceptualization.

Nanqi Ren: Supervision, Project Administration.

Declaration of interests

The authors declare that they have no known competing financial interests or personal relationships that could have appeared to influence the work reported in this paper.

Dr. Nanqi Ren, the Editor-in-Chief of *Environmental Science and Ecotechnology*, was not involved in the editorial review or the decision to publish this article.

Acknowledgment

This research was supported by the National Natural Science Foundation of China (No. 52070059)

Appendix A. Supplementary data

Supplementary data to this article can be found online at https://doi.org/10.1016/j.ese.2026.100664.

References

[1] N. Duque, L. Scholten, M. Maurer, When does infrastructure hybridisation outperform centralised infrastructure paradigms? – exploring economic and hydraulic impacts of decentralised urban wastewater system expansion, Water Res. 254 (2024) 121327.
[2] A. Torre, I. Vázquez-Rowe, E. Parodi, R. Kahhat, Wastewater treatment decentralization: is this the right direction for megacities in the global south? Sci. Total Environ. 778 (2021) 146227.
[3] C. Zhang, G. Zhao, Y. Jiao, B. Quan, W. Lu, P. Su, Y. Tang, J. Wang, M. Wu, N. Xiao, Y. Zhang, J. Tong, Critical analysis on the transformation and upgrading strategy of Chinese municipal wastewater treatment plants: towards sustainable water remediation and zero carbon emissions, Sci. Total Environ. 896 (2023) 165201.
[4] H. Fu, J. Niu, Z. Wu, P. Xue, M. Sun, H. Zhu, B. Cheng, Influencing factors of stereotypes on wastewater treatment plants-case study of 9 wastewater treatment plants in Xi'an, China, Environ. Manag. 70 (2022) 526–535.
[5] Y. Bai, A. Xu, Y.-H. Wu, S. Xue, Z. Chen, H.-Y. Hu, Portrait of municipal wastewater of China: inspirations for wastewater collection, treatment and management, Water Res. 277 (2025) 123321.
[6] MOHURC, Statistical Yearbook of Urban and Rural Construction, 2020 (in Chinese).
[7] D. Zhang, X. Dong, S. Zeng, X. Wang, D. Gong, L. Mo, Wastewater reuse and energy saving require a more decentralized urban wastewater system? Evidence from multi-objective optimal design at the city scale, Water Res. 235 (2023) 119923.
[8] W. Zhu, C. Duan, B. Chen, Energy efficiency assessment of wastewater treatment plants in China based on multiregional input–output analysis and data envelopment analysis, Appl. Energy 356 (2024) 122462.
[9] I. Ribarova, V. Vasilaki, E. Katsou, Review of linear and circular approaches to on-site domestic wastewater treatment: analysis of research achievements, trends and distance to target, J. Environ. Manag. 367 (2024) 121951.
[10] X. Pan, Y. Zhao, X. Lin, N. Zhao, M. Sun, J. Ma, Towards sustainable urban water system: a strategic approach to advance decarbonizing water management, Engineering 50 (2025) 31–39.
[11] M. Molinos-Senante, M. Poch, D. Rosso, M. Garrido-Baserba, From wastewater treatment plants to decentralized resource factories, npj Clean Water 7 (2024) 46.
[12] P.P. Kalbar, S. Lokhande, Need to adopt scaled decentralized systems in the water infrastructure to achieve sustainability and build resilience, Water Policy 25 (2023) 359–378.
[13] S. Lokhande, P.P. Kalbar, A method for appropriate sizing of sewerage zones from sustainability and resilience perspectives using scaled decentralization, J. Environ. Manag. 387 (2025) 125904.
[14] Y. Zhang, Z. Wang, J. Hu, C. Pu, Intelligent management of carbon emissions of urban domestic sewage based on the internet of things, Environ. Res. 251 (2024) 118594.
[15] R. Liu, Y. Ma, H. Zhang, D. Han, X. Hao, S. Li, X. Geng, A review-based estimation of GHG emissions of China's wastewater management system, J. Environ. Manag. 380 (2025) 124869.
[16] H. Muzioreva, T. Gumbo, N. Kavishe, T. Moyo, I. Musonda, Decentralized wastewater system practices in developing countries: a systematic review, Util. Policy 79 (2022) 101442.
[17] L.P.B. Cabling, Y. Kobayashi, E.G.R. Davies, N.J. Ashbolt, Y. Liu, Life cycle assessment of community-based sewer mining: integrated heat recovery and fit-for-purpose water reuse, Environments 7 (2020) 36.
[18] H. Appiah-Twum, T. Van Winckel, J. Santolin, J. De Paepe, S. Hellweg, T.A. Larsen, K.M. Udert, S.E. Vlaeminck, M. Spiller, Environmental impact of integrating decentralized urine treatment in the urban wastewater management system: a comparative life cycle assessment, Water Res. 282 (2025) 123630.
[19] R. Zhang, Z. Wang, Z. Cao, D.P.L. Rousseau, S.V. Hulle, Addressing the rural wastewater treatment dilemma: a techno-environmental-economic analysis, Chem. Eng. J. 504 (2025) 158905.
[20] E. Risch, C. Boutin, P. Roux, Applying life cycle assessment to assess the environmental performance of decentralised versus centralised wastewater systems, Water Res. 196 (2021) 116991.
[21] Y. Kobayashi, N.J. Ashbolt, E.G. Davies, Y. Liu, Life cycle assessment of decentralized greywater treatment systems with reuse at different scales in cold regions, Environ. Int. 134 (2020) 105215.
[22] A.H. Sabeen, Z.Z. Noor, N. Ngadi, S. Almuraisy, A.B. Raheem, Quantification of environmental impacts of domestic wastewater treatment using life cycle assessment: a review, J. Clean. Prod. 190 (2018) 221–233.
[23] M. Garrido-Baserba, S. Vinardell, M. Molinos-Senante, D. Rosso, M. Poch, The economics of wastewater treatment decentralization: a techno-economic evaluation, Environ. Sci. Technol. 52 (2018) 8965–8976.
[24] H.Y. Hu, N. Goto, K. Fujie, Statistical analyses of operating conditions and power consumption characteristics in small-scale conventional activated sludge plants for sewage treatment, Environ. Technol. 21 (2000) 1167–1172.
[25] J. Yang, B. Chen, Energy efficiency evaluation of wastewater treatment plants (WWTPs) based on data envelopment analysis, Appl. Energy 289 (2021) 116680.
[26] I. Roefs, B. Meulman, J.H. Vreeburg, M. Spiller, Centralised, decentralised or hybrid sanitation systems? Economic evaluation under urban development uncertainty and phased expansion, Water Res. 109 (2017) 274–286.
[27] P. Song, Y. Li, H. Chen, L. Li, H. Xia, Y. Xiao, B. Fang, Y. Guo, Z. Bai, L. Ma, Characterization of sewage quality and its spatiotemporal variations in a small town in Eastern Guangdong, China, Front. Water 5 (2024) 1278336.
[28] A. Khajavian, A. Pourmohamadi, Y. Khatibi, S. Nazif, Static calibration of wastewater treatment plant models: investigating calibration processes and objective functions, J. Water Proc. Eng. 54 (2023) 104016.
[29] Y. Gao, X. Shi, X. Jin, X.C. Wang, P. Jin, A critical review of wastewater quality variation and in-sewer processes during conveyance in sewer systems, Water Res. 228 (2023) 119398.
[30] A. Torre, I. Vázquez-Rowe, E. Parodi, R. Kahhat, A multi-criteria decision framework for circular wastewater systems in emerging megacities of the Global South, Sci. Total Environ. 912 (2024) 169085.
[31] S. Hube, T. Zaqout, Ó. Ögmundarson, H.Ó. Andradóttir, B. Wu, Constructed wetlands with recycled concrete for wastewater treatment in cold climate: performance and life cycle assessment, Sci. Total Environ. 904 (2023) 166778.
[32] R. Liu, Y. Zhao, L. Doherty, Y. Hu, X. Hao, A review of incorporation of constructed wetland with other treatment processes, Chem. Eng. J. 279 (2015) 220–230.
[33] M.-J. José Carlos de, B. Patrícia Camara de, R.P. Ribeiro, D.C. Kligerman, J.L.M. Oliveira, Nitrogen removal and nitrous oxide emission from moving bed biofilm reactor (MBBR) under different loads and airflow, J. Environ. Chem. Eng. 12 (2024) 112574.
[34] X. Xing, X. Yuan, Y. Zhang, C. Men, Z. Zhang, X. Zheng, D. Ni, H. Xi, J. Zuo, Enhanced denitrification of the AO-MBBR system used for expressway service area sewage treatment: a new perspective on decentralized wastewater treatment, J. Environ. Manag. 345 (2023) 118763.
[35] L. Corominas, D.M. Byrne, J.S. Guest, A. Hospido, P. Roux, A. Shaw, M.D. Short, The application of life cycle assessment (LCA) to wastewater treatment: a best practice guide and critical review, Water Res. 184 (2020) 116058.
[36] S. Morera, L. Corominas, M. Rigola, M. Poch, J. Comas, Using a detailed inventory of a large wastewater treatment plant to estimate the relative importance of construction to the overall environmental impacts, Water Res. 122 (2017) 614–623.
[37] J.D. Resende, M.A. Nolasco, S.A. Pacca, Life cycle assessment and costing of wastewater treatment systems coupled to constructed wetlands, Resour. Conserv. Recycl. 148 (2019) 170–177.
[38] J. Willis, B. Brower, W. Graf, S. Murthy, C. Peot, P. Regmi, K. Sharma, Z. Yuan, New GHG methodology to estimate/quantify sewer methane, odors and air pollutants conference, Water Environ. Federat. (2018) 562–569, 2018.
[39] H. Zhou, L. Wei, D. Wang, W. Zhang, Environmental impacts and optimizing strategies of municipal sludge treatment and disposal routes in China based on life cycle analysis, Environ. Int. 166 (2022) 107378.
[40] X. Hao, X. Wang, R. Liu, S. Li, M.C.M. van Loosdrecht, H. Jiang, Environmental impacts of resource recovery from wastewater treatment plants, Water Res. 160 (2019) 268–277.
[41] P.K. Cornejo, Q. Zhang, J.R. Mihelcic, How does scale of implementation impact the environmental sustainability of wastewater treatment integrated with resource recovery? Environ. Sci. Technol. 50 (2016) 6680–6689.
[42] H. Xu, G. Fu, Q. Ye, M. Lyu, X. Yan, Life cycle environmental impacts of urban water systems in China, Water Res. 266 (2024) 122350.
[43] E. Twagirayezu, L. Fan, X. Liu, A. Iqbal, X. Lu, X. Wu, F. Zan, Comparative life cycle assessment of sewage sludge treatment in wuhan, China: sustainability evaluation and potential implications, Sci. Total Environ. 913 (2024) 169686.
[44] IEA, Net Zero by 2050, IEA, Paris, 2021. https://www.iea.org/reports/net-zero-by-2050. Licence: CC BY 4.0.
[45] R.R.Z. Tarpani, A. Azapagic, Life cycle costs of advanced treatment techniques

for wastewater reuse and resource recovery from sewage sludge, J. Clean. Prod. 204 (2018) 832–847.
[46] M. Garrido-Baserba, I. Barnosell, M. Molinos-Senante, D.L. Sedlak, K. Rabaey, O. Schraa, M. Verdaguer, D. Rosso, M. Poch, The third route: a techno-economic evaluation of extreme water and wastewater decentralization, Water Res. 218 (2022) 118408.
[47] N. Duque, L. Scholten, M. Maurer, Exploring transitions of sewer wastewater infrastructure towards decentralisation using the modular model TURN-sewers, Water Res. 257 (2024) 121640.
[48] A. Abulimiti, X. Wang, N. Ren, Exploring the pathway for the energy-environment synergistic WWTPs through comprehensive efficiency assessment, J. Water Proc. Eng. 76 (2025) 108269.
[49] J. Chen, F. Guo, F. Wu, B.A. Bryan, Costs and benefits of constructed wetlands for meeting new water quality standards from China's wastewater treatment plants, Resour. Conserv. Recycl. 199 (2023) 107248.
[50] D.J. Dürrenmatt, O. Wanner, A mathematical model to predict the effect of heat recovery on the wastewater temperature in sewers, Water Res. 48 (2014) 548–558.
[51] R. Negi, M.K. Chandel, Life cycle assessment of wastewater reuse alternatives in urban water system, Resour. Conserv. Recycl. 204 (2024) 107469.
[52] IPCC, Refinement to the 2006 IPCC Guidelines for National Greenhouse Gas Inventories, Intergovernmental Panel on Climate Change, Switzerland, 2019, 2019.
[53] H.E. Jijingi, S.K. Yazdi, Y.A. Abakar, E. Etim, Evaluation of membrane bioreactor (MBR) technology for industrial wastewater treatment and its application in developing countries: a review, Case Stud. Chem. Environ. Eng. 10 (2024) 100886.
[54] X. Yang, V. López-Grimau, Reduction of cost and environmental impact in the treatment of textile wastewater using a combined MBBR-MBR system, Membranes 11 (2021) 892.
[55] Q. Zhang, Y. Yang, X. Zhang, F. Liu, G. Wang, Carbon neutral and techno-economic analysis for sewage treatment plants, Environ. Technol. Innov. 26 (2022) 102302.
[56] R. Bhattacharya, D. Mazumder, Performance evaluation of moving bed bioreactor for simultaneous nitrification denitrification and phosphorus removal from simulated fertilizer industry wastewater, Environ. Sci. Pollut. Control Ser. 30 (2023) 49060–49074.
[57] G. Mannina, K. Chandran, M. Capodici, A. Cosenza, D. Di Trapani, M.C.M. van Loosdrecht, Greenhouse gas emissions from membrane bioreactors: analysis of a two-year survey on different MBR configurations, Water Sci. Technol. 78 (2018) 896–903.
[58] J.A. Kawan, H.A. Hasan, F. Suja, O. Jaafar, R. Abd-Rahman, A review on sewage treatment and polishing using moving bed bioreactor (MBBR), J. Eng. Sci. Technol. 11 (2016) 1098–1120.
[59] F. Pasciucco, I. Pecorini, R. Iannelli, Planning the centralization level in wastewater collection and treatment: a review of assessment methods, J. Clean. Prod. 375 (2022) 134092.
[60] W. Chen, Y. Bai, W. Zhang, S. Lyu, W. Jiao, Perceptions of different stakeholders on reclaimed water reuse: the case of Beijing, China, Sustainability 7 (2015) 9696–9710.
[61] N. Funamizu, M. Iida, Y. Sakakura, T. Takakuwa, Reuse of heat energy in wastewater: implementation examples in Japan, Water Sci. Technol. 43 (2001) 277–285.
[62] D. Lang, Y. Qiu, H. Yan, Z. XiaWu, L. Shanshan, W. Jian, Feasibility study on eliminating septic tanks in mountainous cities, Water & Wastewater Eng. 60 (2024) 99–103.
[63] X. Wang, Y. Tian, H. Liu, X. Zhao, Q. Wu, Effects of influent COD/TN ratio on nitrogen removal in integrated constructed wetland–microbial fuel cell systems, Bioresour. Technol. 271 (2019) 492–495.
[64] L. Wushang, G. Jingyang, Z. Chunwei, Z. Lijin, Z. Lifen, D. Xin, Study on methane emission processes from gravity sewers in two cities of Southern and Northern China, Water & Wastewater Eng. 60 (2024) 127–137+145.
[65] Y. Liu, B.-J. Ni, K.R. Sharma, Z. Yuan, Methane emission from sewers, Sci. Total Environ. 524 (2015) 40–51.
[66] R. Boiocchi, M. Mainardis, E.C. Rada, M. Ragazzi, S.C. Salvati, Trends of N2O production during decentralized wastewater treatment: a critical review, J. Environ. Chem. Eng. 13 (2025) 114627.
[67] A. Abulimiti, X. Wang, J. Kang, L. Li, D. Wu, Z. Li, Y. Piao, N. Ren, The trade-off between N_2O emission and energy saving through aeration control based on dynamic simulation of full-scale WWTP, Water Res. 223 (2022) 118961.
[68] P. Sudalaimuthu, R. Sathyamurthy, U. Ali, Renewable hydrogen production steps up wastewater treatment under low-carbon electricity sources – a call forth approach, Desalination Water Treat. 320 (2024) 100748.
[69] J. Du, Y. Laghari, Y.-C. Wei, L. Wu, A.-L. He, G.-Y. Liu, H.-H. Yang, Z.-Y. Guo, S.J. Leghari, Groundwater depletion and degradation in the North China plain: challenges and mitigation options, Water 16 (2024) 354.
[70] Y. Xu, Y. Huang, N. Jiang, M. Song, X. Xie, X. Xu, Experimental and theoretical study on an air-source heat pump water heater for northern China in cold winter: effects of environment temperature and switch of operating modes, Energy Build. 191 (2019) 164–173.